ORIGINAL ARTICLE

WILEY **Cancer Science**

Curcumin analog, GO-Y078, overcomes resistance to tumor angiogenesis inhibitors

Kazuhiro Shimazu[1] | Masahiro Inoue[1] | Shunsuke Sugiyama[2] | Koji Fukuda[1] | Taichi Yoshida[1] | Daiki Taguchi[1] | Yoshihiko Uehara[3] | Sei Kuriyama[4] | Masamitsu Tanaka[4] | Masatomo Miura[5] | Hiroshi Nanjyo[6] | Yoshiharu Iwabuchi[7] | Hiroyuki Shibata[1] (iD)

[1]Department of Clinical Oncology, Graduate School of Medicine, Akita University, Akita, Japan

[2]Sugiyama Clinic, Kurokawa, Miyagi, Japan

[3]Faculty of Health Sciences, Butsuryo College of Osaka, Osaka, Japan

[4]Department of Molecular Medicine and Biochemistry, Akita University, Akita, Japan

[5]Department of Pharmacy, Akita University Hospital, Akita, Japan

[6]Department of Clinical Pathology, Akita University Hospital, Akita, Japan

[7]Department of Organic Chemistry, Graduate School of Pharmaceutics, Tohoku University, Sendai, Japan

Correspondence: Hiroyuki Shibata, Department of Clinical Oncology, Akita University, Graduate School of Medicine, Hondo 1-1-1, Akita 010-8543, Japan (hiroyuki@med.akita-u.ac.jp).

Tumor angiogenesis inhibition is one of the most potent strategies in cancer chemotherapy. From past clinical studies, inhibition of the vascular endothelial growth factor pathway successfully treats malignant tumors. However, vascular endothelial growth factor inhibitors alone cannot cure tumors. Moreover, resistance to small molecule inhibitors has also been reported. Herein, we show the antiangiogenic potential of a newly synthesized curcumin analog, GO-Y078, that possibly functions through inhibition of actin stress fiber formation, resulting in mobility inhibition; this mechanism is different from that of vascular endothelial growth factor inhibition. In addition, we examined the detailed mechanism of action of the antiangiogenesis potential of GO-Y078 using human umbilical venous epithelial cells resistant to angiogenesis inhibitors (HUVEC-R). GO-Y078 inhibited the growth and mobility of HUVEC-R at 0.75 μmol/L concentration. Expression analyses by microarray and RT-PCR showed that expressions of genes including that of *fibronectin 1* were significantly suppressed. Among these genes, *fibronectin 1* is abundantly expressed and, therefore, seems to be a good target for GO-Y078. In a knockdown experiment using Si-oligo of *fibronectin 1* (*FN1*), *FN1* expression was decreased to half of that in mock experiments as well as GO-Y078. Knockdown of *FN1* resulted in the suppression of HUVEC-R growth at 24 hours after treatment. Fibronectin is a key molecule contributing to angiogenesis that could be inhibited by GO-Y078. Thus, resistance to vascular endothelial growth factor inhibition can be overcome using GO-Y078.

KEYWORDS

angiogenesis inhibitor, curcumin analog, fibronectin, sorafenib, sunitinib

1 | INTRODUCTION

Antiangiogenic therapy is one of the potent strategies for treating advanced cancers. Several successful cases treated with this therapy

have been reported so far; for example, bevacizumab has been used for VEGF inhibition[1] and ramucirumab for the inhibition of its type 2 receptor.[2] These monoclonal antibodies can control the growth of cancers, such as advanced colorectal,[3] gastric,[4] lung,[5] ovarian,[6] and brain[7] malignancies. Small molecules, such as sorafenib[8] and sunitinib,[9] which show multiple kinase inhibitory activities, can suppress VEGF receptors (VEGFR) and inhibit tumor angiogenesis. They are also effective in treating advanced hepatocellular carcinoma,[10] renal cell carcinoma,[11] and gastrointestinal stromal tumors.[12] However, contrary to our expectations, the potential of these inhibitors to inhibit the VEGF pathway is insufficient in completely controlling cancer cell growth.[13] One possible explanation for this ineffectiveness is the redundancy of the angiogenesis pathway, which can bypass VEGF inhibition. Tumor angiogenesis can be stimulated by various other pathways, including fibroblast growth factor,[14] PDGF,[15] and hepatocyte growth factor[16] pathways. However, use of these pathways involves the problem of acquired resistance to inhibitors.[17] Recently, we showed the antiangiogenic potential of a newly synthesized curcumin analog, GO-Y078.[18] This diarylpentanoid has the following formula: (1E,4E)-1-(4-hydroxy-3,5-dimethoxyphenyl)-5-(3,4,5-trimethoxyphenyl)-penta-1,4-dien-3-one. Curcumin has an antiangiogenic effect through the inhibition of the VEGF pathway.[19] However, the mechanism underlying the antiangiogenic effect of GO-Y078 is entirely different from that of VEGF inhibition; for instance, GO-Y078 suppresses angiogenesis through the inhibition of actin stress fiber formation.[18] This effect contributes to the stacking of vascular endothelia and induction of anoikis. In this regard, it is important to identify the precise mechanisms underlying this phenomenon. Furthermore, considering that GO-Y078 can inhibit angiogenesis through other pathways besides the VEGF pathway, we hypothesized that it can overcome the problem of resistance to VEGF inhibitors, such as sorafenib and sunitinib.

2 | MATERIALS AND METHODS

2.1 | Cell lines

Human umbilical vein endothelial cells (HUVEC) were obtained from Takara Bio Inc. (Otsu, Japan). Resistant HUVEC (HUVECKi2, Ki4, and Ki5) were kindly gifted by Professor Kazuto Nishio of Kindai University (Osaka, Japan).[20] The cells were cultured using EGMTM-2 Bullet Kit (Takara Bio Inc., Otsu, Japan), which contains 2% FBS, 0.04% hydrocortisone, 0.4% human fibroblast growth factor basic, 0.1% VEGF, 0.1% R3-insulin-like growth factor 1, 0.1% ascorbic acid, 0.1% human epidermal growth factor, 0.1% amphotericin B, and 0.1% heparin (Becton Dickinson and Company, Franklin Lakes, NJ, USA), unless otherwise specified. Human CTCL cell line HH of ATCC was purchased from Summit Pharmaceutical International (Tokyo, Japan).

2.2 | Compounds

GO-Y078, GO-Y030, GO-Y022, and GO-Y136 were synthesized as previously described[21-23] (Figure 1). Wako special grade curcumin was purchased from Wako Pure Chemical Industries, Ltd (Osaka, Japan). Curcumin and its analogs were dissolved in DMSO (Wako Pure Chemical Industries, Ltd) and diluted at final concentrations of 0.002%-0.1%. Sunitinib, sorafenib, and Ki8751, which are selective VEGFR-2 inhibitors, were purchased from Sigma-Aldrich (St Louis, MO, USA), LC Laboratories (Woburn, MA, USA), and Wako Pure Chemical Industries, Ltd, respectively.

2.3 | Cell growth assay

Growth-suppressive effects of the test compounds were measured for 72 hours, as previously described.[22] All cellular experiments were conducted in triplicate unless otherwise specified. Growth curves were obtained using the following protocol: HUVECKi2 was seeded at 0.5×10^5 cells to each well in a 96-well plate and counted at each time interval as indicated.

2.4 | Wound-healing assay

Detailed method of the wound-healing assay was previously described.[18] Briefly, 2×10^5 cells were inoculated onto 12-well, gelatin-coated microplates (Sekiya Rika Co., Ltd, Tokyo, Japan). Before treatment, the cells were treated for 24 hours with 0.1% FBS in F-12K medium. Cells in the center of the plate were scratched with a 200-μL micropipette tip, as previously described.[18] The medium was then replaced with the EGMTM-2 Bullet Kit. Next, the cells were incubated with the test compounds in the presence of human recombinant VEGF-A165 (7.5 ng/mL; Wako Pure Chemical Industries, Ltd). Wound closure was quantified by measuring the distance from the baseline at 24 hours after treatment.

2.5 | Filamentous actin staining

Filamentous actin (F-actin) was stained with 0.1 μmol/L Acti-stain 488 phalloidin (Cytoskeleton, Inc., Denver, CO, USA), as described elsewhere.[18]

2.6 | Microarray analysis

Human umbilical vein endothelial cells were treated with 0.5 μmol/L GO-Y078 for 72 hours or 0.04% of DMSO as a control. Samples were prepared in triplicate for each condition. Total RNA was extracted using the mirVana miRNA Isolation Kit (Life Technologies, Carlsbad, CA, USA). After qualification, equal amounts from each set were mixed and labeled as GO-Y078-treated and control groups. The analysis was conducted by Filgen Inc. (Nagoya, Japan). Transcripts from both groups were analyzed using CodeLink Human Whole Genome Bioarray (Applied Microarrays, Inc., Tempe, AZ, USA) composed of 57 000 transcripts, including 45 000 known genes. The data were scanned using GenePix 4400A (Molecular Devices Inc., Sunnyvale, CA, USA) and analyzed using CodeLink Expression Analysis v 5.0 (Applied Microarrays, Inc.) after quantile normalization. The microarray data analysis tool (version 3.2; Filgen Inc.) was used for data analysis.
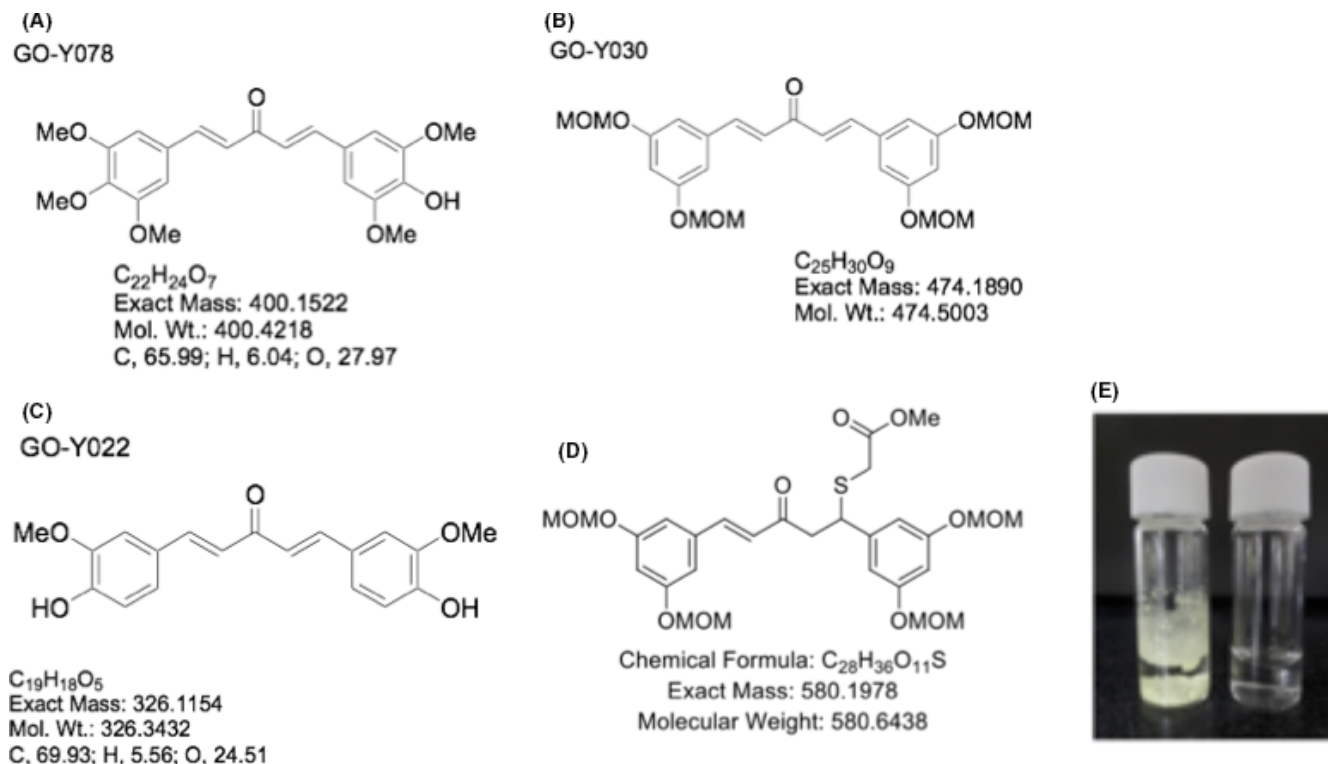
FIGURE 1 Chemical structures of diarylpentanoid curcumin analogs. A, GO-Y078; B, GO-Y030; C, GO-Y022; D, GO-Y136; E, Appearance of 30 mg GO-Y030 (left) and GO-Y136 (right) in PBS

2.7 | Quantitative reverse transcription-polymerase chain reaction

mRNA was obtained from HUVECKi2 incubated without or with 0.5 μmol/L GO-Y078 for 12-36 hours using the NucleoSpin RNA kit (Takara Bio Inc., Shiga, Japan). Complementary DNA was then obtained using the Affinity Script QPCR cDNA Synthesis Kit (Agilent Technologies, Tokyo, Japan), according to the manufacturer's protocol. qPCR was carried out using the LightCycler 480 with LightCycler 480 SYBR Green I Master (Roche Molecular Systems, Inc., Pleasanton, CA, USA). The PCR reaction comprised 3 steps: denaturation (95°C for 10 seconds), annealing (56°C for 10 seconds), and elongation (72°C for 10 seconds).

Expression level of GAPDH was used as the internal control. Relative expression values were corrected using the GAPDH expression values.

The following primers were purchased from Life Technologies Japan Ltd (Tokyo, Japan): FN1(+), 5′-CCATCGCAAACCGCTGCCAT-3′, FN1(−), 5′-AACACTTCTCAGCTATGGGCTT-3′; GAPDH(+), 5′-AAGAAGGTGGTGAAGCAGGC-3′, GAPDH(−), 5′-TCCACCACCCTGTTGCTGTA-3′; ACY1(+), 5′-GGCTGCATGAGGCTGTGTT-3′, ACY1(−), 5′-CTTGGCACTGGTTGGGATG-3′; GNPTG(+), 5′-CAGACTCTGCCAGTCTTTGC-3′, GNPTG(−), 5′-CTCCCACTCGTGCCAGAT-3′; PCSK7(+), 5′-GCAATGGCACCTGAATAACC-3′, PCSK7(−), 5′-GTGGTTGCCATTCTCCACAT-3′; TIMM10B(+), 5′-CTGCGTGACTTCCTGTTGGTC-3′, TIMM10B(−), 5′-TGCGATGCGGCGCTGTACC-3′; ACTR1B(+), 5′-AGCTGGCTTTGCAGGAGACC-3′, ACTR1B(−), 5′-ATGGGTAGCGGATGGTCAGC -3′.

2.8 | Enzyme-linked immunosorbent assay

Enzyme-linked immunosorbent assay was carried out for fibronectin using the Abcam Human Fibronectin ELISA Kit (ab108847; Abcam Japan, Tokyo, Japan), according to the manufacturer's procedures. Briefly, cells were seeded onto each well at a concentration of 0.5×10^5 cells, and the supernatant was corrected at the indicated time with or without GO-Y078.

2.9 | Small interfering RNA transfection

Small interfering RNAs for FN1 were obtained from OriGene Technologies, Inc. (Rockville, MD, USA) and included 3 types of FN-1 siRNA: SR301640A (FN1-A), SR301640B (FN1-B), and SR301640C (FN1-C); SR30004 (mock) was used as a negative control. The siRNAs were transfected with Lipofectamine RNAiMAX transfection reagent (Invitrogen, Tokyo, Japan) according to the manufacturer's protocol. The siRNAs were used at 100-200 nmol/L concentration. Cells that were seeded or were in suspension were next lipofected for 24 hours.

2.10 | Measurement of GO-Y078 concentration in the media

The specimen was applied to an Oasis HLB extraction cartridge (Nihon Waters K.K., Tokyo, Japan) preactivated with methanol and water (1.0 mL each). The cartridge was then washed with 1.0 mL water and 1.0 mL of 80% methanol in water and eluted with 1.0 mL

of 100% methanol. The eluate was dried by vortex-vacuum evaporation at 70°C using a rotary evaporator (AS-ONE CVE-2AS; AS ONE Corporation, Osaka, Japan). The resulting residue was then dissolved in 20 μL methanol and vortexed for 30 seconds; 20 μL of the mobile phase was added to the sample, and the sample was vortexed for another 30 seconds. A 20 μL aliquot of the sample was then processed by HPLC, which was conducted using a PU-2080 plus chromatography pump (JASCO, Tokyo, Japan) equipped with the CAPCELL PAK C18 MG II (250 mm × 4.6 mm i.d.; Shiseido, Tokyo, Japan) HPLC column, a UV-2075 light source, and an ultraviolet detector (JASCO). The mobile phase was acetonitrile-water (65:35, v/v), which was degassed in an ultrasonic bath before use. Flow rate was maintained at 0.5 mL/min at an ambient temperature, and sample detection was carried out at 330 nm.

2.11 | Animal experiments

In vivo experiment was conducted using *Xenopus laevis*, as described previously.[18]

A CTCL cell line, HH, was inoculated in the skin of nude mice, BALB/cA-nu/nu at 5×10^7 cell concentration at each site. On the 7th day after inoculation, GO-Y078 was applied daily as an ointment mixed with petroleum jelly (0.5% w/w) to the tumors formed. After 2 weeks of treatment, the mice were killed and the tumors were analyzed immunohistochemically. Empty petroleum jelly alone was used as a control. Immunohistochemistry was conducted with anti-CD34 antibody (QBEnd/10; Roche Diagnostics K.K., Tokyo, Japan) by using BenchMark ULTRAIHC/ISH Staining Module (Ventana Medical Systems, Inc., Tucson, AZ, USA) according to the manufacturer's protocol. All animal experimental protocols were approved by the Institutional Animal Care and Use Committee at Akita University, and the experiments were conducted in accordance with the Guidelines for Animal Experiments of Akita University (a-1-2503 for *Xenopus* and 23-1-21 for CTCL).

2.12 | Statistical analyses

Stat Mate III (ATMS, Tokyo, Japan) was used to carry out Fisher's exact test. Level of statistical significance was set at $P < .05$.

3 | RESULTS

3.1 | Overcoming the resistance to VEGF inhibitors using diarylpentanoid GO-Y078

Ki8751-resistant clones in HUVECs (HUVECKi cells) were established by Nishio, and the main mechanisms of resistance were downregulation of *VEGF receptors* (*VEGFR1*, *2*, and *3*), which are the targets of VEGF inhibitors. Growth inhibitory effects of GO-Y078 on the VEGF inhibitor-resistant HUVECKi2 were examined. As shown in Figure 2A, GO-Y078 inhibited the growth of HUVECKi2 at concentrations of <1 μmol/L, whereas Ki8751 could not suppress HUVECKi2 at concentrations of approximately 10 μmol/L. Ki8751 is a selective and strong VEGFR-2 inhibitor, and 50% of VEGF signaling is inhibited at 0.9 nmol/L

concentration.[24] IC_{50} of HUVECKi2 for GO-Y078 was 1.0 μmol/L. In addition, sorafenib was slightly sensitive for HUVECKi2; however, its IC_{50} value was 6.3 μmol/L (Figure 2A). IC_{50} values of Ki8751 and sunitinib were 17.0 and 16.5 μmol/L, respectively. For HUVECKi2, GO-Y078 was 17.0-, 16.7-, and 6.4-fold more sensitive an inhibitor than Ki8751, sunitinib, and sorafenib, respectively. For primary HUVEC, the IC_{50} values of GO-Y078, Ki8751, sorafenib, and sunitinib were 0.6, 0.9, 1.5, and 2.2 μmol/L, respectively. HUVECKi2 was 1.7-, 18.9-, 4.2-, and 7.5-fold more resistant than HUVEC for GO-Y078, Ki8751, sorafenib, and sunitinib, respectively (Table S1). For the other VEGF inhibitor-resistant HUVECKi cells, HUVECKi4 and HUVECKi5, we also examined the effects of GO-Y078 (Figure S1 and Table S1). The antiangiogenic potential of GO-Y078 was equal to that of either VEGF inhibitor-resistant or VEGF inhibitor-sensitive cells. The IC_{50} values of GO-Y078 were 1.6 and 1.3 μmol/L for HUVECKi4 and HUVECKi5, respectively. The IC_{50} values of sorafenib were 2.8 and 3.5 μmol/L for HUVECKi4 and HUVECKi5, respectively. However, Ki8751 and sunitinib did not reach the IC_{50} value of <10 μmol/L for both HUVECKi4 and HUVECKi5. For HUVECKi4, GO-Y078 was 6.25-fold more sensitive than Ki8751 and sunitinib, and 1.8-fold more sensitive than sorafenib. For HUVECKi5, GO-Y078 was >7.7-fold more sensitive than Ki8751 and sunitinib, and 2.7-fold more sensitive than sorafenib. GO-Y078 was the most sensitive inhibitor to 3 VEGF inhibitor-resistant HUVECKi cell lines as compared with 3 VEGF inhibitors.

3.2 | Inhibitory effect of GO-Y078 on the mobility of VEGF inhibitor-resistant HUVECKi2

We examined the effect of GO-Y078 on the mobility of VEGF inhibitor-resistant HUVECKi2 using a wound-healing assay. The average distances covered by HUVECKi2 at 0.5 and 1.0 μmol/L GO-Y078 concentrations at 12 hours were 620 ± 18 and 641 ± 9 nm, respectively, whereas it was 505 ± 18 nm without GO-Y078 (Figure 2C,D). The mobile distance was significantly decreased in the presence of 0.5 μmol/L GO-Y078. Furthermore, the mobility distance regressed to −38 ± 29 and −213 ± 22 nm at 24 hours for each GO-Y078 concentration, respectively. These data indicated that several HUVECKi2 were killed or detached in the presence of GO-Y078.

Then, we examined the effect of GO-Y078 on actin stress fiber formation in HUVECKi2 cells. Actin stress fiber formation was inhibited with 1.0 μmol/L GO-Y078 (Figure S2).

3.3 | Microarray analysis

We determined the molecular targets for GO-Y078. Transcription analysis was conducted on the mRNAs derived from the primary HUVEC treated without or with GO-Y078 using microarrays composed of 57 000 transcripts, and the results were compared between the cells treated without or with GO-Y078. The results are shown as the ratios against the mock (without GO-Y078; Figure 3, Table S2). The top 3 transcripts with decreased and increased expressions are described below: Expressions of *aminoacylase-1* (*ACY1*), *FN1*, and *N-acetylglucosamine-1-phosphate transferase gamma*

FIGURE 2 Effect of GO-Y078 on HUVEC resistant to angiogenesis inhibitors. A, Growth inhibition of HUVECKi2 with GO-078 (open rectangle), sorafenib (closed rectangle), sunitinib (closed circle), and Ki8751 (open circle). B, Growth property of HUVECKi2 without (closed circle) and with 1.0 μmol/L GO-Y078 (open circle). *$P < .001$. C, Wound healing assay of HUVECKi2 with GO-Y078. D, Graphical view of the inhibition of the mobility of HUVECKi2. Open, shaded, and closed bars indicate treatments with mock, 0.5 μmol/L, and 1.0 μmol/L, respectively. *$P < .001$, **no significance
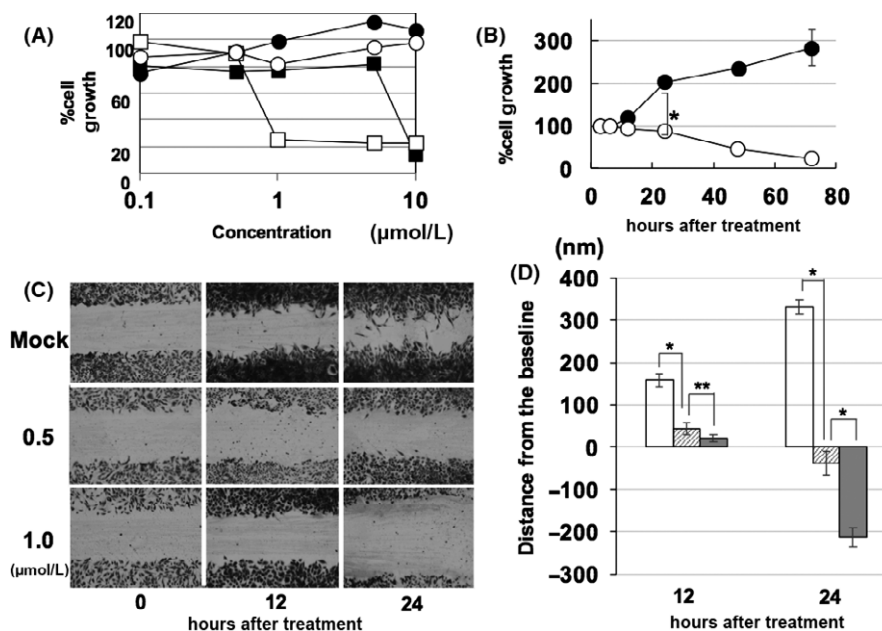
subunit (*GNPTG*) were downregulated because of GO-Y078 to 0.00001-, 0.025-, and 0.025-fold those of the mock, respectively. Conversely, the expressions of *proprotein convertase subtilisin/kexin type 7* (*PCSK7*), *translocase of inner mitochondrial membrane 10B* (*TIMM 10B*), and *ARP1 actin-related protein 1 homolog B* (*ACTR1B*) were upregulated to 124 000-, 10 200-, and 90 100-fold those of the mock, respectively. We considered these genes to be the targets of GO-Y078 for its antiangiogenic potential.

3.4 | Target validation

To confirm the results of microarray analyses, we conducted qRT-PCR for *ACY1*, *FN1*, *GNPTG*, *PCSK7*, *TIMM 10B*, and *ACTR1B* using the cDNAs obtained from HUVECKi2 treated without or with GO-Y078. Relative amounts of the transcripts at baseline, as compared with *GAPDH*, were negligible, except for *FN1*; relative amounts of *ACY1*, *GNPTG*, *PCSK7*, *TIMM 10B*, and *ACTR1B* were 0.00056, 0.000049, 0.0022, 0.0044, and 0.011, respectively, whereas the relative amount of *FN1* was 1.39 (Figure 4A). We next examined the changes in the transcript amounts with 0.5 μmol/L GO-078. Surprisingly, all 5 transcripts, except *TIMM 10B*, were downregulated (Figure 4B). The ranges of the changes were also extremely small, except for *FN1*. As a result, we focused on the expression of *FN1*. The relative expression of *FN1* was suppressed because of GO-Y078 in a dose-dependent way (Figure 5). Relative amounts of *FN1* were 0.39 ± 0.02 and 0.31 ± 0.03 in the presence of 0.5 and 1.0 μmol/L GO-Y078, respectively. Expression of *FN1* was suppressed to 69% of that of the control at 1.0 μmol/L.

3.5 | Downregulation of fibronectin with GO-Y078

We examined the expression of fibronectin encoded by *FN1* in HUVECKi2 treated with GO-Y078 (Figure 6). In the mock treatment, expression level of soluble fibronectin gradually increased from

6 hours after seeding and reached 1.7-fold greater than the baseline value at 24 hours. However, 1.0 μmol/L GO-Y078 significantly suppressed the increased soluble fibronectin at 48 hours after treatment. Under this condition, level of soluble fibronectin reached only 1.8-fold greater than that at 24 hours. However, treatment with 0.5 μmol/L GO-Y078 could not suppress the level of soluble fibronectin. We also examined the suppressive effects of 1.0 μmol/L sorafenib and 1.0 μmol/L sunitinib on soluble fibronectin. Sunitinib slightly reduced the level of soluble fibronectin to 13% of the mock, but sorafenib did not affect the soluble fibronectin levels.

3.6 | Knockdown of *FN1* in VEGF inhibitor-resistant HUVECKi2 cells

The knockdown effect of *FN1* on VEGF inhibitor-resistant HUVECKi2 was investigated using the siRNA technique. The knockdown experiment was conducted using 3 commercially available siRNAs of *FN1*: *Si-FN1A*, *Si-FN1B*, and *Si-FN1C*. First, we transfected siRNAs into seeded HUVECKi2. Among the 3 siRNAs, approximately 50% of knockdown of the *FN1* mRNA expression was achieved by *Si-FN1B* (Figure 7A). Under this condition, we examined the growth of HUVECKi2. As shown in the figure, only a slight delay of growth at 24 hours after treatment was observed (Figure 7B). At 48 hours, the growth delay was recovered. Fibronectin is a deposited extracellular matrix protein secreted by the cells. As fibronectin already exists in the adherent cells, we transfected Si-oligo into the suspended HUVECKi2 to prevent the effect of the preexisting fibronectin. In this case, a maximum of 20% of knockdown of the *FN1* mRNA expression was achieved by *Si-FN1B* (Figure 7C). However, 50% of the growth suppression was apparent in the case of HUVECKi2 transfected by *Si-FN1B* at 24 hours as compared with that in mock transfection (Figure 7D). However, this effect did not last for long and was reversed at 48 hours. Thus, the knockdown of
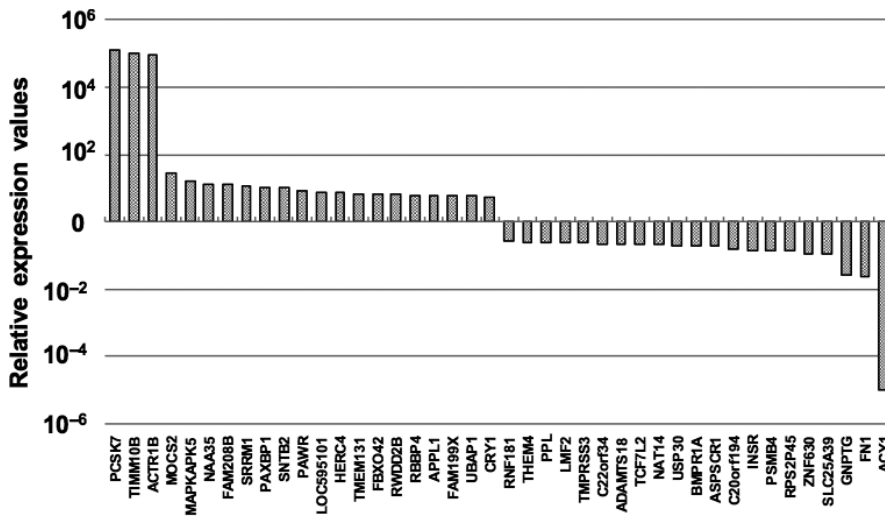
FIGURE 3 Summary of the microarray analysis of HUVEC treated by GO-Y078
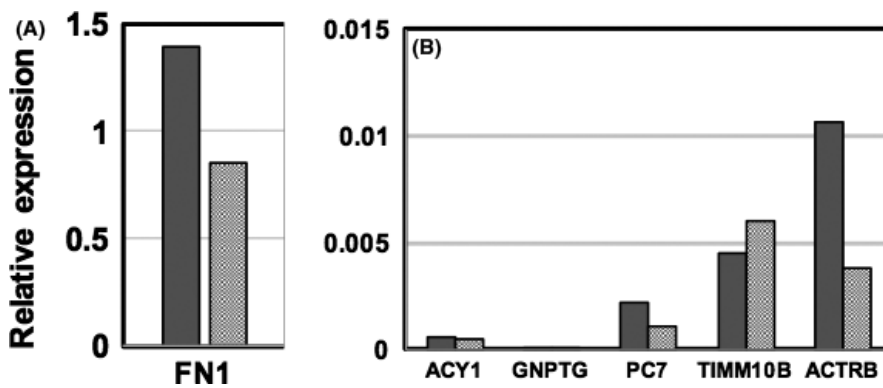

FIGURE 4 RT-PCR of the candidate transcripts in HUVECKi2 affected by GO-Y078. Relative expression values of the basal levels (closed bars) and those of the treated levels with 0.5 μmol/L GO-Y078 (shaded bars) are indicated. A, fibronectin 1 (FN1); B, other candidates
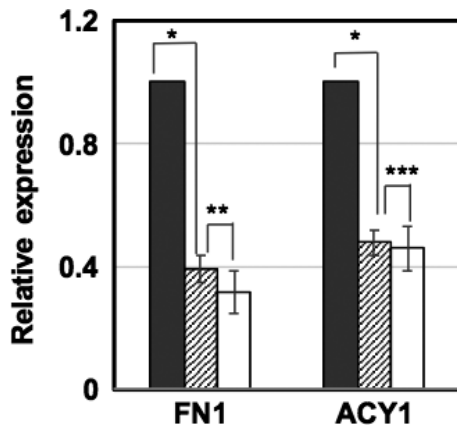

FIGURE 5 Dose-dependent inhibition of *fibronectin 1* (*FN1*) by GO-Y078. Relative expression values of the Mock (indicated by closed bars) and those of the treated levels with 0.5 μmol/L (shaded bars) and 1.0 μmol/L GO-Y078 (open bars) are indicated. *$P < .001$, **$P < .05$. ***no significance

FIGURE 6 Kinetic inhibition of *fibronectin 1* (*FN1*) in HUVECKi2. Relative amount of fibronectin is indicated at each time (h) after treatment. HUVECKi2 was treated with 0.5 μmol/L GO-Y078 (closed rectangle), 1.0 μmol/L GO-Y078 (closed triangle), 1.0 μmol/L sorafenib (closed circle), and 1.0 μmol/L sunitinib (open rectangle). Mock is indicated by open circle. *$P < .05$, **$P < .001$

FN1 could only transiently suppress the growth of HUVECKi2. However, the downregulation of fibronectin with 1.0 μmol/L GO-Y078 lasted for over 48 hours, as shown in Figure 6. The effect of *Si-FN1B* was apparent during 24 hours, but it started to recover at 48 hours (Figure S3A). The suppressive effect of GO-Y078 on HUVECKi2 could be sustained for a long time. HPLC analysis of GO-
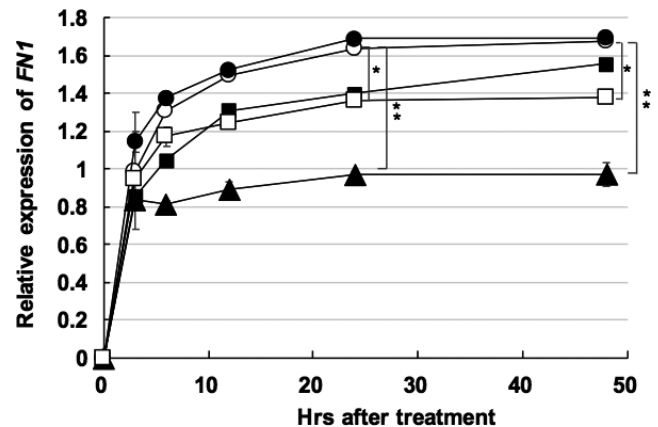
Y078 indicated that once it was added to the medium, the concentration gradually decreased, but $65.5\% \pm 3.15\%$ of the initial concentration was maintained in the medium (Figure S3B). This is a possible reason for the difference in inhibition between *Si-FN1B* and GO-Y078. We found that fibronectin is a key molecule contributing to

FIGURE 7 Knockdown effect of *fibronectin 1* (*FN1*) on the growth of HUVECKi2. A, Efficacies of Si-oligos to *FN1* mRNA in the attached HUVECKi2. B, Effects on the growth of the attached HUVECKi2 treated with *FN1*-Si-oligo (open circle), control-Si-oligo (closed rectangle), and without Si-oligo (closed circle). C, Efficacies of Si-oligos to *FN1* mRNA in the suspended HUVECKi2. D, Effects of the growth of the suspended HUVECKi2 treated with the *FN1*-Si-oligo (open circle), control-Si-oligo (closed rectangle), and without Si-oligo (closed circle)
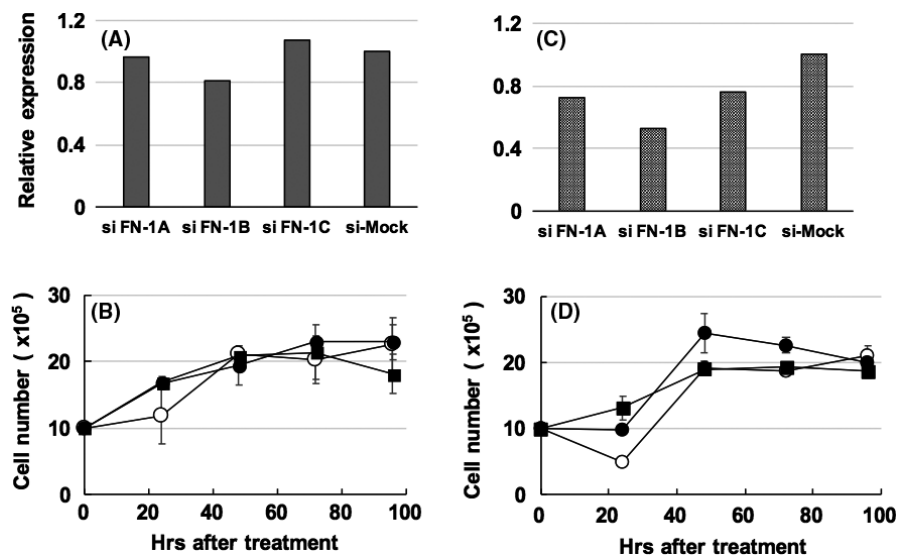
angiogenesis and that it could be inhibited by GO-Y078. It was thus speculated that the resistance to VEGF inhibition can be overcome with GO-Y078, partially as a result of fibronectin suppression.

3.7 | In vivo antiangiogenic effects of GO-Y078

As shown previously, GO-Y078 inhibits angiogenesis in the developing tadpole of *Xenopus*, such as vascular branching and posterior cardinal vein defects (Figure S4).[18] Sunitinib and sorafenib induced angiogenesis abnormalities in 66.7% and 17.3% of the treated fetuses at 1.0 μmol/L, respectively. In the curcumin and mock treatments, abnormalities were observed in 10% and 18.7% at 1.0 μmol/L, respectively. In GO-Y078 treatment, the frequency of angiogenesis abnormalities was 50% at the same concentration. We also examined the inhibition of tumor angiogenesis with GO-Y078 in nude mice inoculated with CTCL cell line HH. VEGF regulates tumor angiogenesis of CTCL.[25] Use of GO-Y078 ointment could significantly inhibit the angiogenesis surrounding the skin tumors as well as skin tumor apoptosis (Figure S5). Microvessel density was $1.7 \pm 0.6/mm^2$ in mock CTCL, whereas it was $0.7 \pm 0.3/mm^2$ ($P = 0.0002$) in CTCL tumor treated with GO-Y078.

3.8 | Optimization of GO-Y078

It has been shown that GO-Y078 has a new antitumor angiogenic potential through the inhibition of actin stress fiber formation by FN1 downregulation. Thus, we examined the antiangiogenic potential of the other DCA. Among them, topical uses of GO-Y030 and GO-Y022 show antitumor potential in vivo.[26] GO-Y030 showed comparable antiangiogenic potential to GO-Y078. IC50 values of GO-Y030 for primary HUVEC, HUVECKi2, and HUVECKi4 were 0.7, 0.8, and 0.4 μmol/L, respectively (Table S1 and Figure S1). However, GO-Y022 was less effective than GO-Y078 and GO-Y030. The IC50 values of GO-Y022 were 3.4, 2.9, and 1.8 μmol/L, respectively. However, these values of DCA, even that of GO-Y022, were much lower than those of the angiogenic inhibitors such as Ki8751, sunitinib,

and sorafenib (Table S1). We next examined the effects on actin stress fiber formation with DCA in HUVEC and resistant HUVECKi (Figure S2D). In the presence of DCA, the cell density of the treated HUVEC and resistant HUVECKi was very low as compared with that of the control. These cells could not stretch their cell body well because of the inhibition of actin stress fiber formation by DCA. However, these DCA cannot be dissolved in water and their bioavailability is low. Recently, we successfully developed a series of water-soluble forms from GO-Y030 by conjugating bis-thiol-adduct to GO-Y030 (Figure 1).[23] GO-Y136 is the most potent derivative bearing antitumor potential. The IC50 value of GO-Y136 was 0.8, 1.6, and 0.7 μmol/L for primary HUVEC, HUVECKi2, and HUVECKi4, respectively (Table S1). These values were comparable with those of GO-Y078 and GO-Y030. GO-Y136 could also inhibit actin stress fiber formation such as GO-Y078 and GO-Y030 (Figure S2D). GO-Y136 is bioavailable and can be used i.v.

4 | DISCUSSION

In our previous study,[18] we showed that GO-Y078 does not affect VEGF signaling but that it affects actin organization and focal adhesion of HUVEC. In the present study, we indicated that GO-Y078 can inhibit the growth of HUVECKi2, 4, and 5, which are resistant to VEGF signaling inhibitors, such as Ki8751, sunitinib, and sorafenib. This finding is consistent with that of a previous report that suggested actin organization-dependent migration of HUVEC as a critical step in the inhibition and as a target for treatment, although angiogenesis is controlled by upstream growth factors. The direct targets or specific underlying mechanisms of angiogenesis inhibition due to GO-Y078 remain to be elucidated. We analyzed the expression profile of HUVEC treated with GO-Y078 using microarray analysis. Among the transcripts affected by GO-Y078, *FN1* expression was decreased, and suppression of *FN1* and its products was confirmed by qRT-PCR and ELISA, respectively. Furthermore, knockdown of *FN1* inhibited the growth of HUVECKi2. Inhibition of

fibronectin may contribute to the antiangiogenic effect of GO-Y078 to an extent. Secretion of fibronectin from endothelial cells leads to the migration of these cells and angiogenesis through integrins.[27] A recent report[28] also indicated that angiogenesis is initiated by soluble fibronectin. Fibronectin is believed to be the key target for antiangiogenic treatment. In fact, anastellin that binds to fibronectin inhibits angiogenesis. Superfibronectin, a polymer of fibronectin that enhances its adhesive properties, also inhibits angiogenesis. Collectively, these results suggest that fibronectin is an important target for antiangiogenesis therapy.[29-31] It has also been suggested that fibronectin stimulates actin remodeling and phosphorylation of focal adhesion component in an independent way from VEGF signaling.[32] Fibronectin associates with F-actin through integrins, such as $\alpha5\beta1$ and $\alpha v\beta3$.[33] Downregulation of fibronectin could result in disorganization of F-actin, as observed with GO-Y078 treatment; thus, fibronectin is an important player in angiogenesis. Ki8751 specifically inhibits VEGFR-2 phosphorylation, but sorafenib and sunitinib have multitarget natures. Sunitinib inhibits multiple kinases, including all receptors for PDGF and VEGFR.[9] Sorafenib inhibits multiple kinases, including Raf kinase, PDGF, and VEGFR-2 and VEGFR-3.[8] These agents suppress growth signaling pathways from the upstream receptors. On the contrary, GO-Y078 suppresses different sites of the pathways. GO-Y078 directly suppresses the effectors of angiogenic signaling such as FN1 and actin stress fiber formation (Figure S6). Unlike sunitinib, sorafenib inhibited the growth of the resistant HUVECKi by decreasing the protein levels of FN1 at 2-5 μmol/L.[34,35]

It remains to be determined whether fibronectin is a direct target for GO-Y078. Curcumin and its analogs, such as GO-Y078, may not directly associate with DNA or RNA, but they may associate with various proteins by Michael addition. In the present study, suppression of fibronectin was observed at the transcriptional and the translational levels. GO-Y078 may affect the transcriptional machinery. Our DCA bearing the same chemical structure can directly bind KH type-splicing regulatory protein, which is a single-strand nucleic acid binding protein that affects different species of mRNAs and microRNAs. Preliminary data indicated that GO-Y078 affects microRNAs,[36] some of which are associated with the regulation of fibronectin expression.

GO-Y030 is comparable with GO-Y078. However, neither GO-Y078 nor GO-Y030 dissolves in water and are therefore not suitable for i.v. administration. GO-Y136, a water-soluble form of GO-Y030, can be given i.v., thereby acting as a good agent for systemic usage.

Curcumin and its analogs have multitarget potentials,[37] and they directly affect certain molecules and show some biological reactions. When a biological event is initiated in cells (eg, angiogenesis), the concentrations of proteins that contribute to the process are increased and accumulated within the endothelial cells. Curcumin analogs may associate more frequently with these proteins because of the increased amount of these proteins and then degrade them.[38] It has previously been shown that curcumin could induce degradation of an oncogene product by the Michael reaction acceptor activity.[39] As a result, the cells are transformed back from the active stage to the onset or static stage. Thus, curcumin analogs may merely degrade the excess amount of protein induced by some biological reactions, which could be the effect of their multitarget potential; however, these events remain to be systematically investigated.

CONFLICTS OF INTEREST

Authors declare no conflicts of interest for this article.

ORCID

Hiroyuki Shibata [ID] http://orcid.org/0000-0003-3581-3506

REFERENCES

1. Roviello G, Bachelot T, Hudis CA, et al. The role of bevacizumab in solid tumours: a literature based meta-analysis of randomised trials. *Eur J Cancer*. 2017;75:245-258.
2. Falcon BL, Chintharlapalli S, Uhlik MT, Pytowski B. Antagonist antibodies to vascular endothelial growth factor receptor 2 (VEGFR-2) as anti-angiogenic agents. *Pharmacol Ther*. 2016;164:204-225.
3. Seeber A, Gastl G. Targeted therapy of colorectal cancer. *Oncol Res Treat*. 2016;39:796-802.
4. Samson P, Lockhart AC. Biologic therapy in esophageal and gastric malignancies: current therapies and future directions. *J Gastrointest Oncol*. 2017;8:418-429.
5. Manzo A, Montanino A, Carillio G, et al. Angiogenesis inhibitors in NSCLC. *Int J Mol Sci*. 2017;18:2021.
6. Chase DM, Chaplin DJ, Monk BJ. The development and use of vascular targeted therapy in ovarian cancer. *Gynecol Oncol*. 2017;145:393-406.
7. Trevisan E, Bertero L, Bosa C, et al. Antiangiogenic therapy of brain tumors: the role of bevacizumab. *Neurol Sci*. 2014;35:507-514.
8. Chen J, Jin R, Zhao J, et al. Potential molecular, cellular and microenvironmental mechanism of sorafenib resistance in hepatocellular carcinoma. *Cancer Lett*. 2015;367:1-11.
9. Mena AC, Pulido EG, Guillén-Ponce C. Understanding the molecular-based mechanism of action of the tyrosine kinase inhibitor: sunitinib. *Anticancer Drugs*. 2010;21:S3-S11.
10. Yau T, Chan P, Epstein R, Poon RT. Management of advanced hepatocellular carcinoma in the era of targeted therapy. *Liver Int*. 2009;29:10-17.
11. Randrup Hansen C, Grimm D, Bauer J, Wehland M, Magnusson NE. Effects and side effects of using sorafenib and sunitinib in the treatment of metastatic renal cell carcinoma. *Int J Mol Sci*. 2017;18:E461.
12. Braconi C, Bracci R, Cellerino R. Molecular targets in gastrointestinal stromal tumors (GIST) therapy. *Curr Cancer Drug Targets*. 2008;8:359-366.
13. Rajabi M, Mousa SA. The role of angiogenesis in cancer treatment. *Biomedicines*. 2017;5:E34.
14. Presta M, Chiodelli P, Giacomini A, Rusnati M, Ronca R. Fibroblast growth factors (FGFs) in cancer: FGF traps as a new therapeutic approach. *Pharmacol Ther*. 2017;179:171-187.

15. Heldin CH, Lennartsson J, Westermark B. Involvement of platelet-derived growth factor ligands and receptors in tumorigenesis. *J Intern Med*. 2018;283:16-44.

16. Mo HN, Liu P. Targeting MET in cancer therapy. *Chronic Dis Transl Med*. 2017;3:148-153.

17. Lord S, Funes JM, Harris AL, Quintela-Fandino M. Antiangiogenic resistance and cancer metabolism: opportunities for synthetic lethality. *Curr Drug Targets*. 2016;17:1714-1727.

18. Sugiyama S, Yoshino Y, Kuriyama S, et al. A curcumin analog, GO-Y078, effectively inhibits angiogenesis through actin disorganization. *Anticancer Agents Med Chem*. 2016;16:633-647.

19. Kasi PD, Tamilselvam R, Skalicka-Woźniak K, et al. Molecular targets of curcumin for cancer therapy: an updated review. *Tumour Biol*. 2016;37:13017-13028.

20. Arao T, Matsumoto K, Furuta K, et al. Acquired drug resistance to vascular endothelial growth factor receptor 2 tyrosine kinase inhibitor in human vascular endothelial cells. *Anticancer Res*. 2011;31:2787-2796.

21. Ohori H, Yamakoshi H, Tomizawa M, et al. Synthesis and biological analysis of new curcumin analogues bearing an enhanced potential for the medicinal treatment of cancer. *Mol Cancer Ther*. 2006;5:2563-2571.

22. Kudo C, Yamakoshi H, Sato A, et al. Synthesis of 86 species of 1,5-diaryl-3-oxo-1,4-pentadienes analogs of curcumin can yield a good lead in vivo. *BMC Pharmacol*. 2011;11:4.

23. Kohyama A, Fukuda M, Sugiyama S, et al. Reversibility of the thia-Michael reaction of cytotoxic C5-curcuminoid and structure-activity relationship of bis-thiol-adducts thereof. *Org Biomol Chem*. 2016;14:10683-10687.

24. Kubo K, Shimizu T, Ohyama S, et al. Novel potent orally active selective VEGFR-2 tyrosine kinase inhibitors: synthesis, structure-activity relationships, and antitumor activities of *N*-phenyl-*N'*-{4-(4-quinolyloxy)phenyl}ureas. *J Med Chem*. 2005;48:1359-1366.

25. Miyagaki T, Sugaya M, Oka T, et al. Placental growth factor and vascular endothelial growth factor together regulate tumour progression via increased vasculature in cutaneous T-cell lymphoma. *Acta Derm Venereol*. 2017;97:586-592.

26. Shibata H, Yamakoshi H, Sato A, et al. Newly synthesized curcumin analog has improved potential to prevent colorectal carcinogenesis in vivo. *Cancer Sci*. 2009;100:956-960.

27. Kim S, Bell K, Mousa SA, Varner JA. Regulation of angiogenesis in vivo by ligation of integrin alpha5beta1 with the central cell-binding domain of fibronectin. *Am J Pathol*. 2000;156:1345-1362.

28. Zhou X, Rowe RG, Hiraoka N, et al. Fibronectin fibrillogenesis regulates three-dimensional neovessel formation. *Genes Dev*. 2008;22:1231-1243.

29. Han SW, Roman J. Fibronectin induces cell proliferation and inhibits apoptosis in human bronchial epithelial cells: pro-oncogenic effects mediated by PI3-kinase and NF-kappa B. *Oncogene*. 2006;25:4341-4349.

30. Yi M, Ruoslahti E. A fibronectin fragment inhibits tumor growth, angiogenesis, and metastasis. *Proc Natl Acad Sci USA*. 2001;98:620-624.

31. El-Ayoubi F, Amiral J, Pascaud J, et al. A fibrin antibody binding to fibronectin induces potent inhibition of angiogenesis. *Thromb Haemost*. 2015;113:143-153.

32. Raimondi C, Fantin A, Lampropoulou A, Denti L, Chikh A, Ruhrberg C. Imatinib inhibits VEGF-independent angiogenesis by targeting neuropilin 1-dependent ABL1 activation in endothelial cells. *J Exp Med*. 2014;211:1167-1183.

33. Truong H, Danen EH. Integrin switching modulates adhesion dynamics and cell migration. *Cell Adh Migr*. 2009;3:179-181.

34. Chen YL, Zhang X, Bai J, et al. Sorafenib ameliorates bleomycin-induced pulmonary fibrosis: potential roles in the inhibition of epithelial-mesenchymal transition and fibroblast activation. *Cell Death Dis*. 2013;4:e665.

35. Thabut D, Routray C, Lomberk G, et al. Complementary vascular and matrix regulatory pathways underlie the beneficial mechanism of action of sorafenib in liver fibrosis. *Hepatology*. 2011;54:573-585.

36. Yamakoshi H, Kanoh N, Kudo C, et al. KSRP/FUBP2 is a binding protein of GO-Y086, a cytotoxic curcumin analogue. *ACS Med Chem Lett*. 2010;1:273-276.

37. Hewlings SJ, Kalman DS. Curcumin: a review of its effects on human health. *Foods*. 2017;6:E92.

38. Kudo C, Yamakoshi H, Sato A, et al. Novel curcumin analogs, GO-Y030 and GO-Y078, are multi-targeted agents with enhanced abilities for multiple myeloma. *Anticancer Res*. 2011;31:3719-3726.

39. Jung Y, Xu W, Kim H, Ha N, Neckers L. Curcumin-induced degradation of ErbB2: a role for the E3 ubiquitin ligase CHIP and the Michael reaction acceptor activity of curcumin. *Biochim Biophys Acta*. 2007;1773:383-390.

SUPPORTING INFORMATION

Additional supporting information may be found online in the Supporting Information section at the end of the article.